

<https://doi.org/10.1038/s43247-025-01997-9>

# Satellites reveal different stories of marine heatwaves in the sea-ice-covered pan-Arctic

Check for updates

Xuewei Zhang <sup>1</sup>, Ning Zhao <sup>2</sup>✉, Zhijun Dai <sup>1</sup>✉ & Zhen Han <sup>3</sup>

Satellite observations provide valuable information on the rapidly increasing marine heatwaves over the Arctic Ocean, yet current assessments of these events lack reliability because the satellite-based temperature in ice-covered regions heavily relies on ice conditions. Here we compared the marine heatwaves derived from two commonly used satellite products to evaluate the potential influences of sea ice in the pan-Arctic. We found inconsistent behaviors of marine heatwaves in both mean fields and temporal variations on interannual and seasonal timescales using two datasets, which became even larger in recent years when they showed opposite tendencies over regions with higher ice concentrations (>50%). Our findings revealed our knowledge of marine heatwaves in the Arctic is facing challenges due to the large influences of sea ice and datasets that were ignored in previous studies, highlighting an urgent need for in situ observations and consistent and reliable long-time datasets for the warming Arctic.

The global sea surface temperature (SST) has exhibited a clear warming trend in recent decades<sup>1</sup>, bringing more frequent extremely warm events in the global oceans<sup>2</sup> (i.e., the marine heatwaves, MHWs). These extremely warm events persist for days and months, significantly modulating the marine ecosystems and the related human societies<sup>3–5</sup>. Particularly, some recent studies found that MHWs have increased by about 34% during the last hundred years (1925–2016)<sup>6,7</sup> and could become even more frequent if global warming continues<sup>2</sup>. In addition to the increasing occurrence, longer MHWs also become more common in recent years, resulting in more MHW-dominant days throughout the year<sup>6,8</sup>.

Among the regions undergoing the impact of global warming, the Arctic suffers the most severe changes with a four-times faster SST warming than the globe, which is known as the ‘Arctic amplification’<sup>9–12</sup>. Meanwhile, the decline of the sea ice in the Arctic<sup>13–15</sup> also induces great impacts on the climate and ecosystems<sup>16–18</sup>. Recent studies further demonstrated that the sea ice in the Arctic experienced a clear regime shift to thinner and uniform ice cover in 2007 due to the loss of multiyear ice<sup>19–21</sup>, while simulations further suggest a seasonally ice-free Arctic may appear soon if the warming continues<sup>22</sup>. Because of that, MHWs that were usually mentioned in lower-to-mid latitudes are now a common and ‘hot’ phenomenon in this icy world, showing a certain impact on the ocean state and related ecosystems<sup>23,24</sup>.

Previous studies suggest that MHW activities in the Arctic kept enhancing during the past decades, including their frequency, duration,

intensity, and areal coverage<sup>25,26</sup>, but such a trend was not homogeneously distributed due to the different driving mechanisms<sup>27</sup>. Meanwhile, declining sea ice cover also accelerates Arctic warming and MHW activities by enhancing heat transfer into the ocean<sup>23,28</sup>. Meltwater-induced shallow mixed layers also favor MHW activities<sup>27</sup>, particularly in regions with lower sea ice concentrations (SIC < 50%)<sup>29</sup>.

While the Arctic MHWs have been extensively investigated in many previous studies, most of them were performed using satellite-based SST products<sup>6,30,31</sup>. Although these products provide valuable information that allows the long-term monitoring of the Arctic, few studies have paid attention to their limitations. For example, the satellite-based SSTs heavily rely on the ice conditions not only due to their close physical nature but also because of the unavoidable influences of sea ice on the microwave signals and processing algorithms<sup>32–35</sup>. Meanwhile, different sensors and retrieval algorithms would also generate noticeable differences among the datasets<sup>36,37</sup>, which may have a large uncertainty in our assessments of MHWs and their future changes<sup>38</sup>.

Therefore, in this study, we aim to provide comprehensive estimations of MHWs in the sea-ice-covered pan-Arctic and their temporal variations during the past four decades (1982–2023) by explicitly considering the influences of sea ice and dataset selections on the MHW assessment. To do so, two commonly used satellite SST products were obtained for extracting MHWs and intercomparison: the UK Met Office (0.05°) Operational Sea

<sup>1</sup>State Key Laboratory of Estuarine and Coastal Research, East China Normal University, Shanghai, China. <sup>2</sup>Center for Coupled Ocean-Atmosphere Research, Research Institute for Global Change, Japan Agency for Marine-Earth Science and Technology, Yokosuka, Japan. <sup>3</sup>College of Oceanography and Ecological Science, Shanghai Ocean University, Shanghai, China. ✉e-mail: [zhaoning@jamstec.go.jp](mailto:zhaoning@jamstec.go.jp); [zjdai@sklec.ecnu.edu.cn](mailto:zjdai@sklec.ecnu.edu.cn)

Surface Temperature and Sea Ice Analysis (OSTIA)<sup>33,39</sup> and the National Oceanic and Atmospheric Administration (NOAA) 0.25° daily Optimum Interpolation SST dataset (OISST)<sup>32,40</sup>. According to our results, the SSTs in the two datasets did not show similar behaviors with the presence of sea ice, while inconsistencies were also found in their sea ice data. As a result, although both datasets suggested enhanced MHW activities in the sea-ice-covered pan-Arctic, we revealed the inconsistent behaviors of MHWs derived from the two datasets on both interannual and seasonal timescales. Larger discrepancies were observed in the recent few years when two datasets exhibited opposite tendencies over ice-rich (SIC > 50%) regions, prohibiting our further conclusion on whether there was a new mode of MHW activity or just algorithm-induced illusions. Moreover, compared to OSTIA, the updates in OISST induced unignorable impacts on the SST performance in ice-covered regions, which greatly influenced the MHWs based on it.

## Results and discussion

### Revisit SSTs with the presence of sea ice

Our first issue in this study is to reveal how SSTs vary in the ice-covered regions in these two commonly used satellite products. Figure 1 shows the mean SSTs and their variances under different sea ice conditions in the pan-Arctic calculated with their original resolutions. In general, SSTs gradually decreased from 2–3 °C to –1.8 °C (the lowest temperature in both datasets) as the SIC increased, and similar negative correlations were found in their variances. Specifically, when the SIC became larger than 50%, the SST and its variance would reduce below 0 °C and 1 °C<sup>2</sup>, respectively, until they became almost constant values in regions fully covered by sea ice (i.e., SIC > 95%).

Furtherly, it was found that the temperatures in OISST were 0.5–1 °C higher than those in OSTIA under most ice conditions<sup>41</sup> until the update of version 2.1 in 2016, which replaced the old linear proxy SST-ice regression by the new salinity-related freezing point algorithm<sup>40</sup>. After that, the reduced SSTs were likely to increase again in 2021, which might be related to the recent update in 2021 when the AVHRR-only OISST began to use both AVHRR and VIIRS data from the NOAA Advanced Clear Sky Processor for Ocean (ACSPO) satellite SSTs<sup>36</sup>. Compared to that, the variability of SSTs in OISST behaved in a different way, which had much higher variances than those in OSTIA but was greatly reduced from 2004. Moreover, in contrast to the regions with less ice, variances of SSTs did not change much in the high-SIC regime (>50%) throughout the entire 42 years. The abovementioned changes in OISST were quite clear if we looked at the time series of SSTs at

some individual data points (Fig. 2; also see Supplementary Figs. 1 and 2). It should be noted that although the newly updated proxy SST algorithm was adopted with a lower SIC criterion of 35%, it could not explain the large reduction of SSTs in the regions with SIC ≤ 35% after 2016.

On the other hand, OSTIA has its own issue. As shown in Fig. 1b, an apparent relaxation of the ice-SST correlation was found in OSTIA since 2016, indicated by the slightly increased SST and greatly enhanced variances that favor the MHWs<sup>42</sup>. However, it is challenging to attribute this possible relaxation solely to the decline of sea ice (e.g., Fig. 3), because OSTIA also updated its ice data from the OSI-450 to OSI-430/OSI-430-b from 2016 although the new data is an extension of the old one with the same processing chain and algorithms<sup>39</sup> (see Supplementary Fig. 3 for details). Moreover, no clear signal was seen in the mean SSTs. Therefore, further investigation is required in the future to confirm whether it is a potential regime shift of ice-SST relation<sup>10</sup> or just an illusion induced by the updated ice data. Another notable thing is that the use of near real-time data might be one of the sources of the reduction of SST variance after 2022, although we did not find any obvious inconsistency in mean SSTs or MHW metrics before and after 2022 (e.g., Figs. 1a, 5, and 6).

### Sea ice conditions in different datasets

After the confirmation of ice-SST relations, it is time to evaluate the sea ice data used in two SST datasets (OSTIA and OISST). Figure 3 shows the climatological mean distributions of sea ice in NSIDC (for reference), OSTIA, and OISST along with their temporal variations. All three datasets generally exhibited similar sea ice distributions, with relatively high SICs (>50%) dominating most subregions in the Arctic, except those near the North Atlantic Ocean likely due to the influence of warm currents. SIC rapidly reduced to 0% outside the Arctic till it became rare south of 60°N. In addition, a clear seasonal cycle could be seen in sea ice variations with the maximum sea ice cover in March and minimum in September (Fig. 3g). From a long-term point of view, most Arctic regions experienced a reduction of sea ice coverage due to global warming during the past four decades<sup>43</sup>, except the central Arctic where a weak increasing trend was seen.

Despite the general similarities, some regional discrepancies should not be ignored. Results show that the SIC in OISST presented a weaker decreasing trend in the whole pan-Arctic but with a larger increasing trend in the central Arctic compared to other datasets. This may be attributed to the change of data source from NASA to NCEP since 2005<sup>40</sup>, resulting in an evident change in its

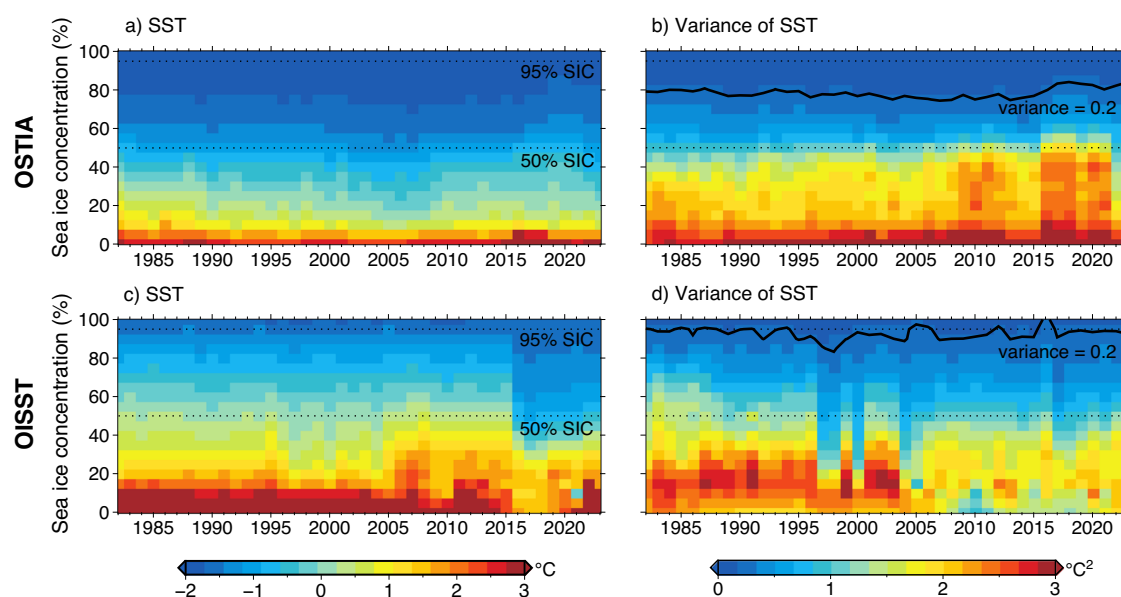
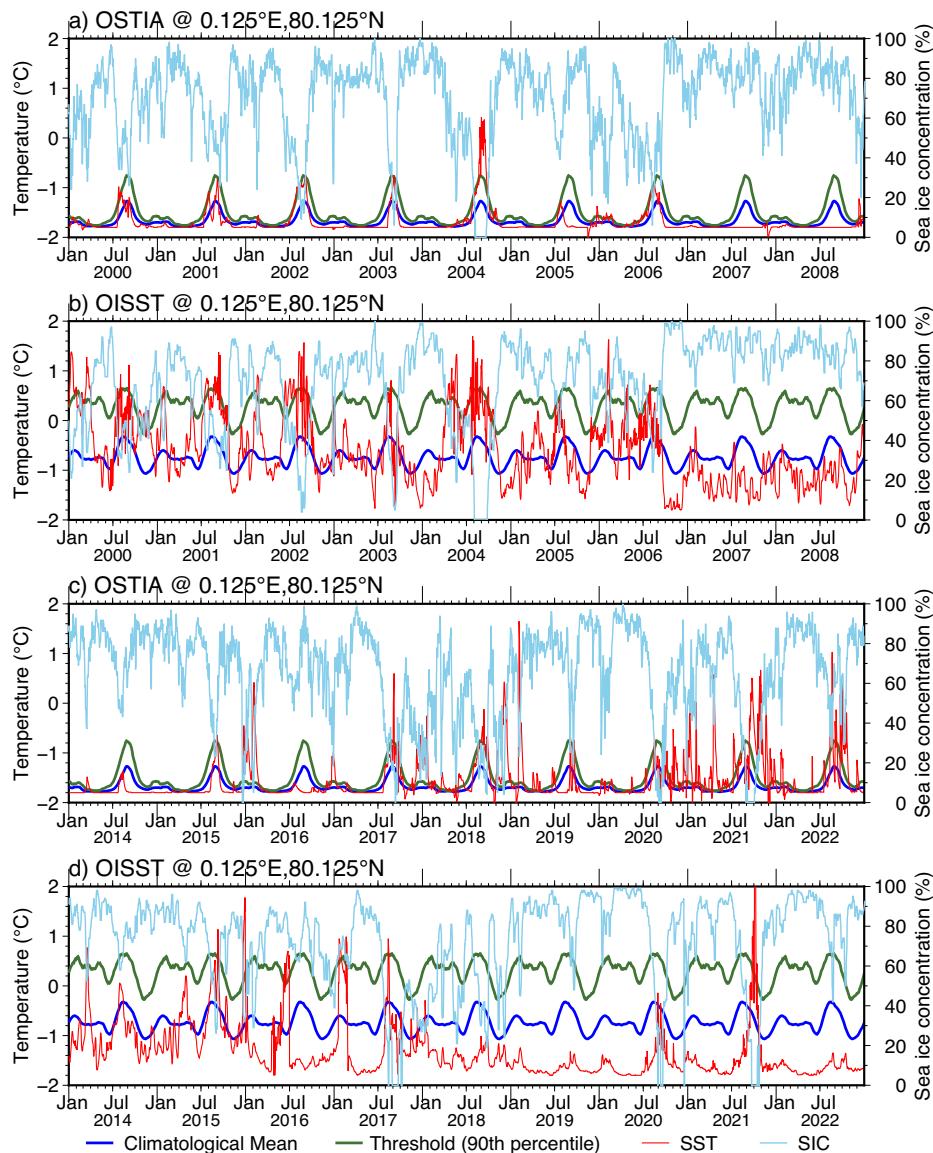


**Fig. 1 | Performances of sea surface temperatures (SSTs) under different sea ice conditions.** Hovmöller-like diagrams for the variations of (a, c) mean temperatures and (b, d) their variances with respect to sea ice concentration (SIC) based on (a, b)

OSTIA and (c, d) OISST. The dotted lines represent the SICs at 50% and 95%, and the black lines in the right panels show the contour of 0.2 SST variance. Results were obtained based on their original resolutions.

**Fig. 2 | An example of SSTs with seasonally varying SIC in OSTIA and OISST at 0.125°E, 80.125°N.** Time series of (red) SST, (blue) 42-year daily climatological mean, (dark-green) thresholds for MHW detection, and (sky-blue) SIC based on (a, c) OSTIA and (b, d) OISST during two 9-year periods: (a, b) 2000–2009 and (c, d) 2014–2022.



variations (Fig. 3i). By contrast, although OSTIA had a larger seasonal amplitude compared to NSIDC (Fig. 3h), they showed good agreement.

More details of sea ice differences could be shown by the area fractions, which were calculated based on a constant total area (defined by the region with climatological mean SIC  $\geq 1\%$ ; also see black contours in Fig. 4) and the similar method for the sea ice extent (Fig. 3j–l). It is found that all three datasets presented an increasing fraction of regions with less ice (SIC  $\leq 50\%$ ), which gradually increased from  $\sim 40\%$  to  $50\%$  during the past 42 years. Note that the sudden reduction of the fraction of ice-free regions (SIC  $\leq 15\%$ ) in OISST was likely induced by the change of ice data source from 2005.

On the other hand, they did not agree well in regions with more ice cover, including most subregions in the pan-Arctic. Data from NSIDC suggested that the high SIC region ( $>95\%$ ) has been declining gradually during the past 42 years, which dominated a large area in the Central Arctic and covered more than half of the Arctic region. Meanwhile, the area of regions with SIC 50–95% remained almost unchanged. In contrast, the two SST products exhibited a much smaller but unchanged high SIC region and a declining area of the regions with SIC 50–95%. One may consider that such different presentations would not be a problem in sea ice assessment; however, it was not the case when considering the SST was strongly influenced by the SIC in satellite products, and lower SICs would allow the existence of higher temperatures and variances and, therefore, influence our estimation of MHWs.

### General characteristics of the pan-Arctic MHWs

Figure 4 presents the extracted metrics of MHWs in the pan-Arctic from 1982 to 2023 based on OSTIA and OISST datasets. In regions without sea ice influence (outside the black contours in Fig. 4), MHWs from both datasets became more active, longer-lasting, and stronger, although OISST-derived MHWs displayed shorter durations and lower intensities than those in OSTIA.

However, with the presence of sea ice (i.e., areas within the black contour in Fig. 4), MHWs behaved quite differently between the two datasets. As shown in Fig. 4a, OSTIA-derived MHWs occurred more frequently in low-SIC marginal seas (e.g., the Greenland Sea and the Barents Sea) and exhibited stronger intensities, likely due to the influences of the North Atlantic current. The mean duration of MHWs ranged from 16 to 20 days with no clear regional dependency except for the central Arctic, where few long-lasting MHWs were seen. Conversely, MHWs derived from OISST are found to be more active across the entire Arctic region even in regions with high SICs in the central Arctic. This could be related to the larger variances found in OISST within the high-SIC regime (e.g., Fig. 1). Moreover, compared to OSTIA, MHWs derived from OISST had an average duration of 4 days shorter, and their mean intensities were also  $1\text{--}2\text{ }^{\circ}\text{C}$  lower.

When looking at the long-term variations, both datasets suggest more and longer-lasting MHWs tended to occur in the regions experiencing faster sea ice decline (Fig. 3), especially in coastal regions of Eurasia. However,

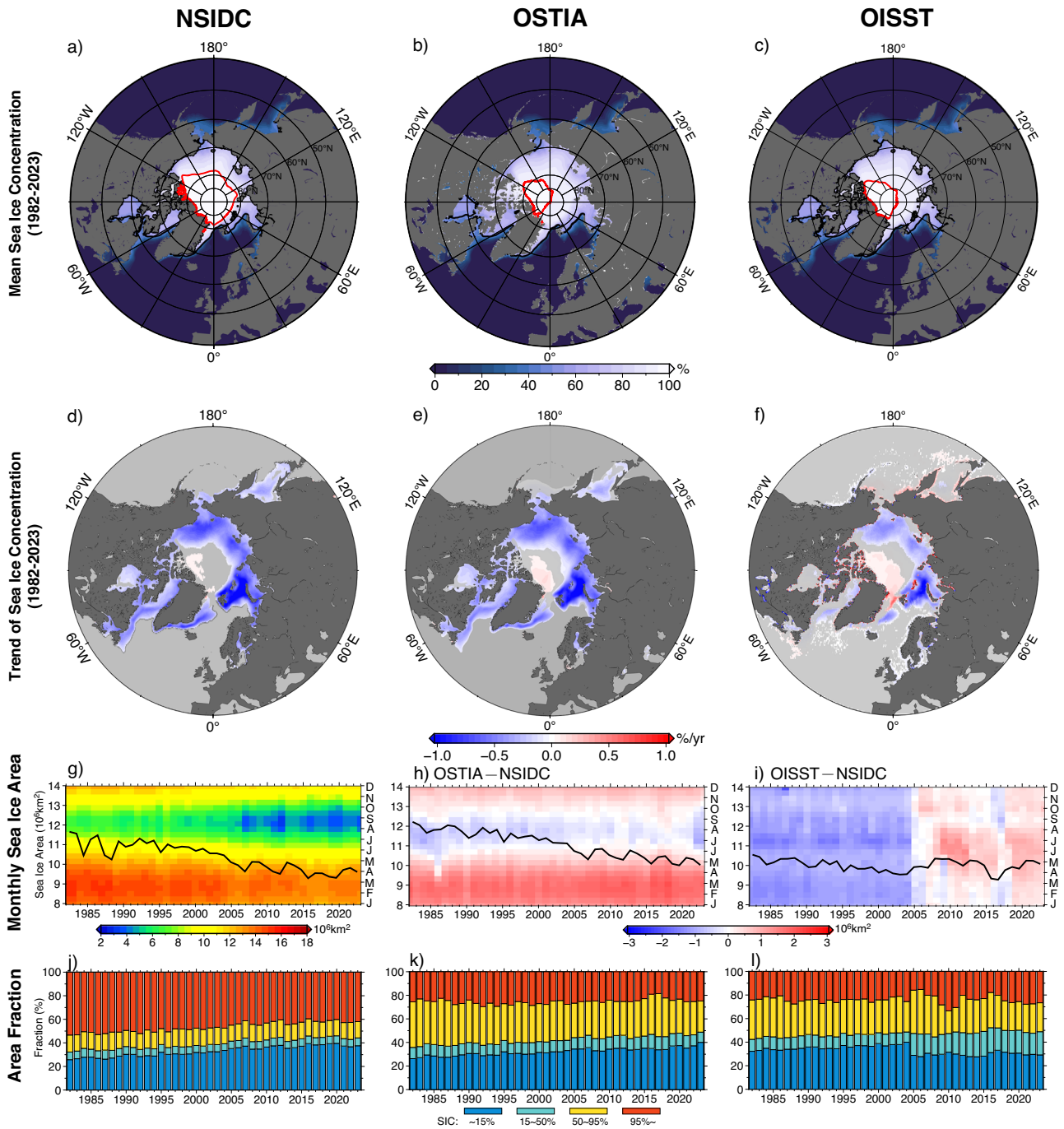


**Fig. 3 | Sea ice conditions in the pan-Arctic.** a–c Mean SIC distributions from 1982 to 2023, d–f their long-term trend, g–i the interannual and seasonal variations of total sea ice area in the pan-Arctic with the annual mean (black lines), and j–l variations of the area fractions for four different ice conditions based on (left

NSIDC, (middle) OSTIA, and (right) OISST. Red and black contours in (a–c) represent the climatological mean 95% and 50% SIC, respectively, and only significant trends ( $p < 0.05$ ) are plotted in (d–f) based on the Mann-Kendall trend test. Results were obtained based on their original resolutions.

their distributions did not match well. It is shown that OSTIA-derived MHWs had a widely distributed and larger increasing trend over the entire Arctic region, but MHWs were limited in the coastal marginal seas only in OISST, which even became fewer in the north of Greenland Island (Fig. 4g, j). In addition to that, even more evident contrasts between the two datasets could be found in the intensities of MHWs, which exhibit opposite signs in their long-term trends, especially for those in the coastal regions (Fig. 4i, l).

**Seasonal and interannual variations of MHWs**

To present the detailed variations of MHWs in the pan-Arctic, Fig. 5 represents the monthly MHW metrics averaged over the ice-covered

regions (i.e., regions inside the black contours in Fig. 4) along with their annual means (black lines). Despite the long-term increasing trends as we mentioned before, MHWs derived by the two datasets did not show many similar variations on both interannual and seasonal timescales. It is found that MHWs derived from OSTIA were quite rare and short-lived in the Arctic before the 2000s, while their occurrence was slightly higher in summer (JJA). After the 2000s, while MHWs tended to occur more often than before and lasted longer, no clear seasonal cycle could be seen except in their intensities.

In contrast to the results based on OSTIA, an MHW-rich Arctic was suggested by OISST, where long-lived (>10 days) MHWs could frequently

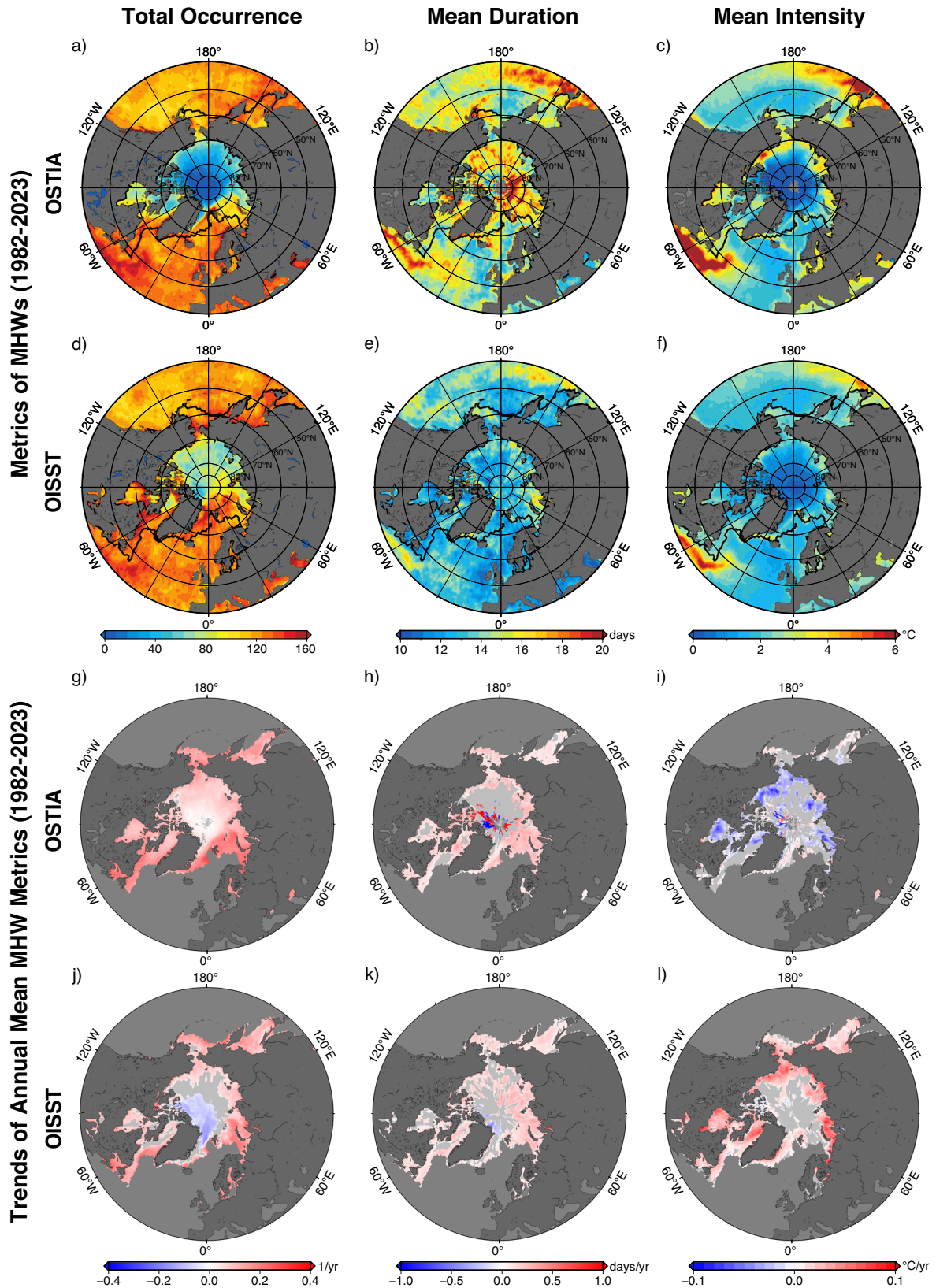


**Fig. 4 | Marine heatwaves (MHWs) in the sea-ice-covered pan-Arctic.** **a, d** Total number of MHWs and **b, e** the mean duration and **c, f** mean intensities of those individual MHWs during the period from 1982 to 2023 based on (a–c) OSTIA and (d–f) OISST. **g–l** Linear trends of annual mean MHW metrics. Black contours in (a–f) represent the target region in this study (climatological mean SIC = 1% in each dataset), and only significant trends ( $p < 0.05$ ) within the target region are plotted in (g–l) based on the Mann-Kendall trend test.

occur in most months since the 1980s even in those with higher SICs (e.g., Fig. 3). Similar to OSTIA, occurrences, and durations of the OISST-derived MHWs did not exhibit any pronounced seasonal cycle but with weak increasing trends since the late 1980s. On the other hand, the OISST-derived MHWs had much lower intensities than those in OSTIA until they were greatly enhanced after 2007.

While the two datasets have already shown discrepancies in the past decades, their differences became even larger in the recent few years. As shown in Fig. 5a, MHWs derived from OSTIA had a rapid increase in their occurrence since 2019 with enhanced MHW activity except in winter, while their durations remained unchanged and intensities became even lower than before. Contrastingly, the MHW activity derived from OISST was suppressed in the spring season after 2017, which was never observed before during the whole study period, although their intensities were enhanced in summer<sup>29</sup>.

Particularly, considering the recent changes in OISST-derived MHWs, it is natural to relate them to the updates adopted in OISST which reduced the mean SSTs and variances (Fig. 1). As shown in Fig. 2 (also see Supplementary Figs. 1, 2), SSTs and their variances became smaller than the years before due to the higher SICs caused by the change of data source (e.g., Fig. 3i). As a result, only the events with extremely high temperatures could exceed the threshold (e.g., Supplementary Fig. 6) and be regarded as MHWs, leading to the large enhancement of their intensities (Fig. 5f). Moreover, such a situation became even clearer after 2016 when the SSTs and variances were further suppressed due to the new freezing point algorithm adopted in version 2.1. Consequently, our results suggest that frequent updates in datasets could greatly influence the long-term variations of SST and MHWs via the modified mean values and variances. Note that, compared to OSTIA, the updates in OISST did correct those unrealistic warm SST biases and variances<sup>41</sup>.

### MHWs under different ice conditions

Our final issue is to confirm whether the sea ice conditions influenced our MHW estimations much. Based on our previous results and for simplicity, we divided the regions in the sea-ice-covered pan-Arctic into two categories: less-ice regions with SICs ≤ 50% and ice-rich regions with 50–95% SICs, while the MHW metrics were obtained accordingly based on their SICs in each month (Fig. 6; also see Supplementary Fig. 4 for seasonal variations).

As shown in Fig. 6, although both datasets suggest the increase of less-ice regions and the reduction of ice-rich regions, their MHWs behaved in a different way. Along with the increasing fractions of less-ice regions (Fig. 3), the MHW activities in both datasets were enhanced continuously during the past four decades. Meanwhile, despite the relatively large interannual variations, a similar increasing trend was also found in their durations. Nevertheless, dramatic changes were observed in the ice-rich regions, which is likely responsible for the previously found changes in recent years. It is suggested that the occurrence of OSTIA-derived MHWs over ice-rich regions was greatly enhanced after 2019 and became almost comparable to those in less-ice regions, which probably caused the reduction in their intensities. By contrast, OISST-derived MHWs almost disappeared in the ice-rich regions during the summer months (MJJA) from 2016 and were also suppressed in other seasons (see Supplementary Fig. 4). Note that the variations of MHWs presented here are consistent with those found in previous studies<sup>29,40</sup>, but we obtained different stories since we used an extended study period.

Although the recent variations of MHW activity in OISST were likely induced by their updates in the data source and algorithm, a similar explanation was not true for OSTIA, because its SST behaved consistently throughout the entire 42-year study period and the previously found relaxation started from 2016 (Fig. 1a, b). Further comparisons of SST and SIC anomalies suggest the increase of MHWs was likely caused by the low sea ice covers from 2019, which allowed the appearance of higher SSTs in the whole Arctic Ocean (see Supplementary Fig. 5), suggesting a potential new mode of MHW activity in the pan-Arctic, especially over the ice-rich regions. However, it should be noted that such a guess requires longer monitoring and more in situ evidence before we could have a clue because the current record is too short compared to the 2-5-year interannual cycles of MHW activities (e.g., Fig. 5).

### Conclusion

In this study, we investigated the complex connections between sea ice and marine heatwaves (MHWs) in the sea-ice-covered pan-Arctic based on 42 years (1982–2023) of two commonly-used satellite SST products, OSTIA and OISST. By comparing the MHWs derived from them, we have

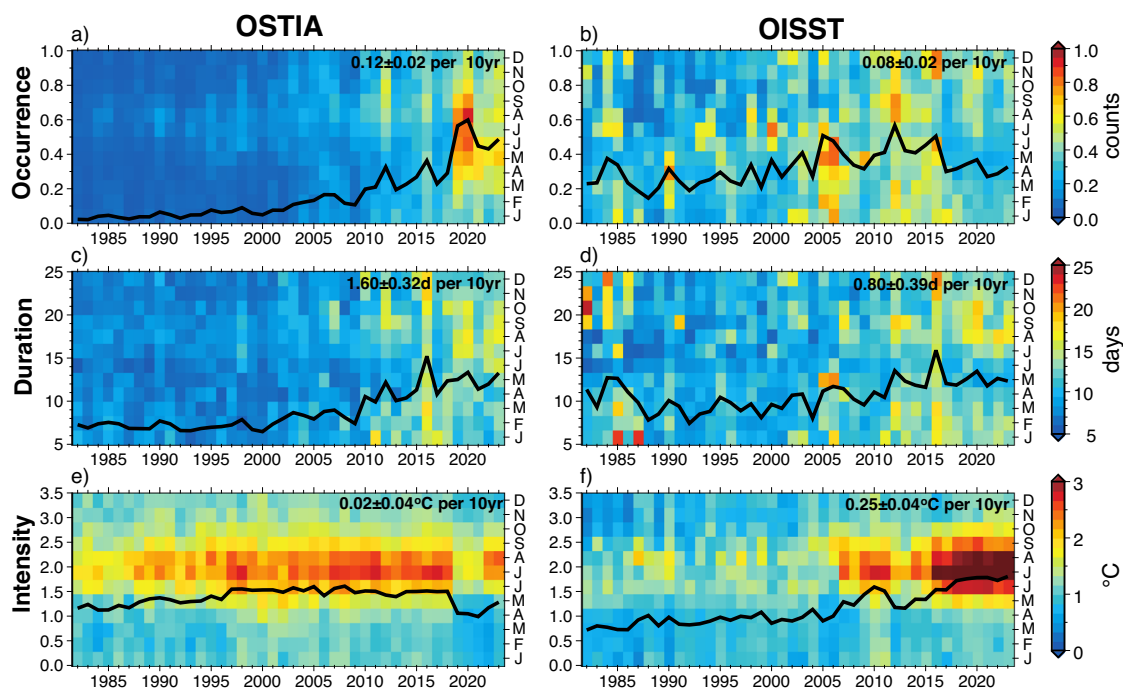


**Fig. 5 | Temporal variation of mean MHW metrics in the sea-ice-covered pan-Arctic.** Interannual (line) and seasonal (color shading) variations of (a, b) the monthly mean MHW occurrence, (c, d) monthly duration, and (e, f) monthly mean

intensity based on (left) OSTIA and (right) OISST. Their linear trends are also embedded in each panel with the upper and lower bounds.

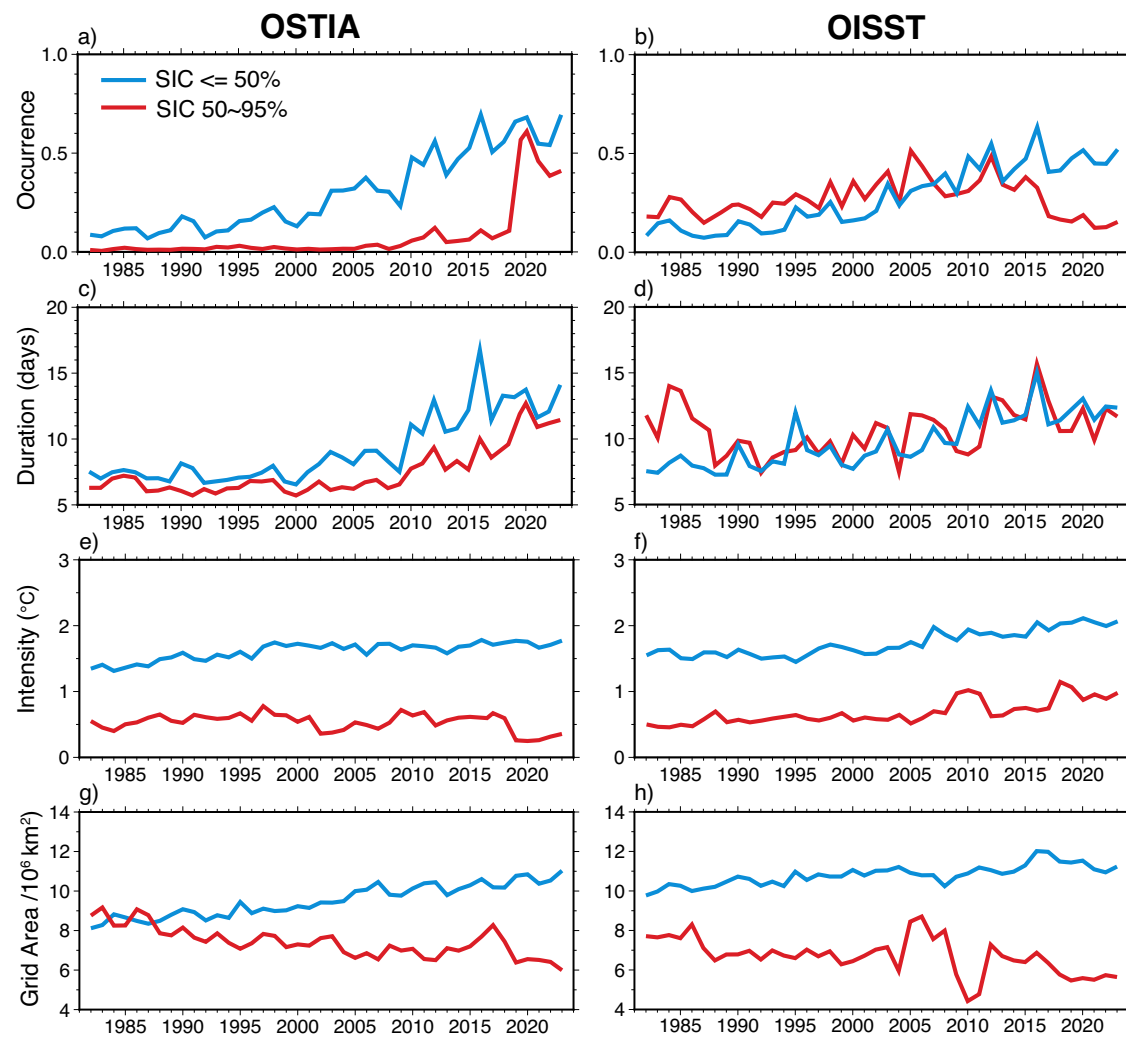


**Fig. 6 | MHWs under different ice conditions in the sea-ice-covered pan-Arctic.** Interannual variations of (a, b) the annual mean MHW occurrence, (c, d) annual duration, (e, f) annual mean intensity, and (g, h) the total grid area based on (left) OSTIA and (right) OISST in regions with (blue) SIC  $\leq 50\%$  and (red) SIC of 50–95%.

demonstrated the large influences of sea ice on MHW characteristics, highlighting the limitations of relying solely on satellite SST data for assessing these extreme events.

While both datasets well represented the mean distributions of sea ice, they did not exhibit similar temporal variations on seasonal and interannual scales. Meanwhile, their different treatment for SSTs in ice-covered regions induced large discrepancies in their MHWs. Although both datasets indicated an intensification of pan-Arctic MHWs, unignorable inconsistencies were observed in their spatial distributions and long-term trends, which were more evident over marginal seas in the pan-Arctic. Moreover, our results also revealed that MHWs in the two datasets experienced entirely different seasonal cycles, except for their similar high intensities in summertime.

In addition, dramatic changes in MHW activities were also observed in the recent few years, as indicated by a rapid enhancement from 2019 in OSTIA and a great suppression from 2017 in OISST. Further analyses suggest that such changes mainly occurred within regions with SICs of 50–95% in both datasets. One possible explanation for the suppression in OISST is their newly updated SST algorithm in v2.1, which reduced the SSTs over ice-covered regions by about 1 °C after 2016. However, it remains unclear whether the enhanced MHW activity in OSTIA was induced by similar technical modifications or the potential shift of the Arctic climate system. Note that extra analyses based on the 0.25° regridDED OSTIA show that our results and conclusions did not rely on the difference between the spatial resolutions of the two datasets.

Our results indicate that our current assessments of MHWs in ice-covered regions are facing challenges due to the large influences of sea ice on the SSTs via both their physical connections and technical issues, suggesting more in situ observations and validations of satellite products are in urgent need. Meanwhile, the results of OISST also remind us that the improved algorithms and sensors may not only make the SST products more reliable but also induce unignorable inconsistencies among their historical archives or different versions, which should be considered and taken into account in climate studies (see an example of long-term baseline comparison in Supplementary Fig. 6).

Finally, it should be claimed that the results of this study are based on only two satellite products and depend on the definition of MHWs. A more reliable and clearer image of the limitations of different satellite sensors/products may be obtained by detailed intercomparison of a wider range of datasets along with their data uncertainties. Moreover, considering the influences of sea ice on the SST analysis, a more practical and proper definition of MHWs in the icy regions should also be considered in future studies.

## Methods

### Data

To investigate MHWs in the ice-covered pan-Arctic, two satellite-based SST products that cover the study period of 1982–2023 were selected (OSTIA and OISST), which have been used in many MHW studies<sup>6,30,31,44</sup>. Meanwhile, the sea ice data embedded in these two datasets were also generated

from satellite observations. OSTIA uses the data from the product OSI-450, OSI-430, OSI-430-b, and OSI-401-b of the Ocean and Sea Ice Satellite Application Facility, while OISST uses the data from the National Aeronautics and Space Administration (NASA; 1981–2004) and the National Center for Environmental Prediction (NCEP; after 2005). Note that we used the reprocessed OSTIA dataset for the data before June 2022 and the near real-time version after that due to their limited temporal coverages during this study. These two datasets were created following the same procedures including the same data assimilation processes and ice analysis<sup>39</sup>, and we did not find obvious inconsistencies between them (e.g. Fig. 1), although the reprocessed dataset includes a wider range of observations.

During our study period, there were several updates were adopted in both two datasets, including the change of satellites, change of ice data, and updated algorithms and schemes<sup>33,36,39,40</sup>. For ease of understanding, a brief timeline diagram is provided in Supplementary Fig. 3 with notable changes in the two datasets.

In this study, the ‘sea-ice-covered’ regions were defined as the 42-year climatological annual mean SIC larger than 1% (see black contour in Fig. 4). To examine the influences of sea ice on the SSTs and its long-term variations in the pan-Arctic, the area of sea ice (grid area multiplied by the SIC) and the sea ice extent (total area of grids with SIC  $\geq$  15%) were calculated using the SIC data combined within the SST products<sup>45</sup>. Moreover, as the reference of sea ice conditions, the monthly 25-km Climate Data Record of Passive Microwave Sea Ice Concentration (V4)<sup>46</sup> is also obtained from the NOAA and the National Snow and Ice Data Center (NSIDC).

### Detection of MHWs

Following previous studies on the Arctic MHWs<sup>23,29</sup>, the definition of heatwaves is based on the seasonally varying 90th percentile threshold of the daily-climatology-removed SST anomalies from 1982 to 2023<sup>47</sup>. Consequently, a heatwave event is defined as a period of warm SST anomaly lasting 5 days or more, and the duration and the mean SST anomaly (i.e., the intensity) are also obtained accordingly. This method was applied to SST datasets (OISST and OSTIA) individually. After that, for ease of inter-comparison and to reduce the potential influences of spurious MHWs or those that have a smaller scale than the eddies in the Arctic region<sup>30,48</sup>, the obtained heatwave metrics were regridded to a  $1^\circ \times 1^\circ$  mesh grid<sup>49</sup>. Moreover, we removed those MHWs when the monthly SIC was larger than 95% because they are less reliable due to the small SST variances<sup>25</sup>, and the month of each MHW was defined by its first occurrence time. Note that this 95% SIC criterion is comparable to those in previous studies<sup>23,25</sup> (see its corresponding SST variance in Fig. 1).

After receiving MHWs under  $1^\circ \times 1^\circ$  uniform grids, the monthly metrics (occurrence, duration, and intensity) were estimated at each grid point to evaluate their temporal variations. It needs to be clarified that the duration of each month is the sum of the heatwave days in each month, and the monthly intensity is also calculated in the same manner but based on the averaged values. Unlike the other two metrics, the occurrence represents the counts of MHWs in a certain area, which needs to be weighted by their grid-cell areas. Moreover, the MHW occurrence would only be counted once in its first month even if it continued in the following months. Finally, to evaluate the MHWs within the sea-ice-covered pan-Arctic and the potential influences of sea ice, we excluded the regions with the 42-year climatological annual mean SIC  $<$  1% or the regions south of  $40^\circ$  N (i.e., outside the black contours in Fig. 4, which represent the climatological mean SIC = 1%).

In addition, one may consider the comparison between OSTIA and OISST in our current procedures is not an apple-to-apple one, because we wish to exhibit their best performance, and the pre-smoothing or averaging of high-resolution data may reduce their advantages. However, such a comparison may result in potential unfairness. Therefore, we also provide the results based on the pre-processed OSTIA, which were regridded from  $0.05^\circ$  to  $0.25^\circ$  by using area-weighted spatial averaging. As shown in Supplementary Figs. 7, 8, and 9, the results of the regridded OSTIA were similar to those obtained using its original resolution, suggesting our results and

related conclusions do not rely on the different resolutions between the datasets.

### Data availability

The data used in this study are listed as follows: the UK Met Office (0.05°) reprocessed (before June 2022) and near real-time (after June 2022) foundation SST from the Operational Sea Surface Temperature and Ice Analysis system (OSTIA; <https://podaac.jpl.nasa.gov/dataset/OSTIA-UKMO-L4-GLOB-REP-v2.0> and <https://podaac.jpl.nasa.gov/dataset/OSTIA-UKMO-L4-GLOB-v2.0>), and the Optimum Interpolation Sea Surface Temperature (OISST; <https://psl.noaa.gov/data/gridded/data.noaa.oisst.v2.highres.html>), and the NOAA/NSIDC monthly 25-km Climate Data Record of Passive Microwave Sea Ice Concentration (V4; <https://nsidc.org/data/g02202/versions/4>). The extracted monthly metrics of marine heatwaves are available at: <https://doi.org/10.5281/zenodo.14552530>.

### Code availability

The MHW detection method is obtained from <https://github.com/ecjoly/marineHeatWaves>. The PyMannKendall package is publicly available at <https://github.com/mmh013/pymannkendall>. All analyses were performed using Python.

Received: 26 August 2024; Accepted: 6 January 2025;

Published online: 10 January 2025

### References

- Cheng, L. et al. An overview of ocean climate change indicators: sea surface temperature, ocean heat content, ocean pH, dissolved oxygen concentration, arctic sea ice extent, thickness and volume, sea level and strength of the AMOC (Atlantic Meridional Overturning Circulation). *Front. Mar. Sci.* **8**, 642372 (2021).
- Frölicher, T. L., Fischer, E. M. & Gruber, N. Marine heatwaves under global warming. *Nature* **560**, 360–364 (2018).
- Cook, F. et al. Marine heat-waves in shallow coastal ecosystems are coupled with the atmosphere: Insights from half a century of daily in situ temperature records. *Front. Clim.* **4**, 1012022 (2022).
- Smale, D. A. et al. Marine heatwaves threaten global biodiversity and the provision of ecosystem services. *Nat. Clim. Change* **9**, 306–312 (2019).
- Smith, K. E. et al. Biological impacts of marine heatwaves. *Annu. Rev. Mar. Sci.* **15**, 119–145 (2023).
- Oliver, E. C. et al. Longer and more frequent marine heatwaves over the past century. *Nat. Commun.* **9**, 1324 (2018).
- Chen, Y. L., Su, H., Yan, X. H., Zhang, H. S. & Wang, Y. P. Global oceans suffer extreme heatwaves intensifying since the early 21st century: a new comprehensive index. *Ecol. Indic.* **162**, 112069 (2024).
- Marin, M., Feng, M., Phillips, H. E. & Bindoff, N. L. A global, multiproduct analysis of coastal marine heatwaves: distribution, characteristics and long-term trends. *J. Geophys. Res. Oceans* **126**, e2020JC016708 (2021).
- Ding, Q. et al. Influence of high-latitude atmospheric circulation changes on summertime Arctic sea ice. *Nat. Clim. Change* **7**, 289–295 (2017).
- Pithan, F. & Mauritsen, T. Arctic amplification dominated by temperature feedbacks in contemporary climate models. *Nat. Geosci.* **7**, 181–184 (2014).
- Rantanen, M. et al. The Arctic has warmed nearly four times faster than the globe since 1979. *Commun. Earth Environ.* **3**, 168 (2022).
- Smetsrud, L. H. et al. Nordic Seas heat loss, Atlantic inflow, and Arctic sea ice cover over the last century. *Rev. Geophys.* **60**, e2020RG000725 (2022).
- Stroeve, J. C., Markus, T., Boisvert, L., Miller, J. & Arrett, A. Changes in Arctic melt season and implications for sea ice loss. *Geophys. Res. Lett.* **41**, 1216–1225 (2014).
- Walsh, J. E., Fetterer, F., Scott Stewart, J. & Chapman, W. L. A database for depicting Arctic sea ice variations back to 1850. *Geogr. Rev.* **107**, 89–107 (2017).

15. Notz, D. & Stroeve, J. Observed Arctic sea-ice loss directly follows anthropogenic CO<sub>2</sub> emission. *Science* **354**, 747–750 (2016).
16. Mori, M., Watanabe, M., Shiogama, H., Inoue, J. & Kimoto, M. Robust Arctic sea-ice influence on the frequent Eurasian cold winters in past decades. *Nat. Geosci.*, **7**, 869–873 (2014).
17. Vihma, T. Effects of Arctic sea ice decline on weather and climate: a review. *Surv. Geophys.* **35**, 1175–1214 (2014).
18. Ardyna, M. & Arrigo, K. R. Phytoplankton dynamics in a changing Arctic Ocean. *Nat. Clim. Change*, **10**, 892–903 (2020).
19. Babb, D. G. et al. The stepwise reduction of multiyear sea ice area in the Arctic Ocean since 1980. *J. Geophys. Res.: Oceans* **128**, e2023JC020157 (2023).
20. Simmonds, I. Comparing and contrasting the behaviour of Arctic and Antarctic sea ice over the 35 year period 1979–2013. *Ann. Glaciol.* **56**, 18–28 (2015).
21. Sumata, H., de Steur, L., Divine, D. V., Granskog, M. A. & Gerland, S. Regime shift in Arctic Ocean sea ice thickness. *Nature* **615**, 443–449 (2023).
22. Serreze, M. C. & Meier, W. N. The Arctic's sea ice cover: trends, variability, predictability, and comparisons to the Antarctic. *Annu. N.Y. Acad. Sci.* **1436**, 36–53 (2019).
23. Barkhordarian, A., Nielsen, D. M., Olonscheck, D. & Baehr, J. Arctic marine heatwaves forced by greenhouse gases and triggered by abrupt sea-ice melt. *Commun. Earth Environ.* **5**, 57 (2024).
24. Kuletz, K. J. et al. Seabird responses to ecosystem changes driven by marine heatwaves in a warming Arctic. *Mar. Ecol. Prog. Ser.* **737**, 59–88 (2024).
25. Huang, B. et al. Prolonged marine heatwaves in the Arctic: 1982–2020. *Geophys. Res. Lett.* **48**, e2021GL095590 (2021).
26. Golubeva, E., Kraineva, M., Platov, G., Iakshina, D. & Tarkhanova, M. Marine Heatwaves in Siberian Arctic Seas and Adjacent Region. *Remote Sens.* **13**, 4436 (2021).
27. Richaud, B. et al. Drivers of marine heatwaves in the Arctic Ocean. *J. Geophys. Res. Oceans* **129**, e2023JC020324 (2024).
28. Dai, A. & Jenkins, M. T. Relationships among Arctic warming, sea-ice loss, stability, lapse rate feedback, and Arctic amplification. *Clim. Dyn.* **61**, 5217–5232 (2023).
29. Hu, S., Zhang, L. & Qian, S. Marine heatwaves in the Arctic region: variation in different ice covers. *Geophys. Res. Lett.* **47**, e2020GL089329 (2020).
30. Bian, C. et al. Oceanic mesoscale eddies as crucial drivers of global marine heatwaves. *Nat. Commun.* **14**, 2970 (2023).
31. Hu, Z.-Z., McPhaden, M. J., Huang, B., Zhu, J. & Liu, Y. Accelerated warming in the North Pacific since 2013. *Nat. Clim. Change* **14**, 929–931 (2024).
32. Reynolds, R. W. et al. Daily high-resolution-blended analyses for sea surface temperature. *J. Clim.* **20**, 5473–5496 (2007).
33. Good, S. et al. The current configuration of the OSTIA system for operational production of foundation sea surface temperature and ice concentration analyses. *Remote Sens.* **12**, 720 (2020).
34. Nielsen-Englyst, P., Høyer, J. L., Alerskans, E., Pedersen, L. T. & Donlon, C. Impact of channel selection on SST retrievals from passive microwave observations. *Remote Sens. Environ.* **254**, 112252 (2021).
35. Vazquez-Cuervo, J. et al. Comparison of GHRSST SST analysis in the Arctic Ocean and Alaskan coastal waters using saildrones. *Remote Sens.* **14**, 692 (2022).
36. Huang, B. et al. Understanding differences in sea surface temperature intercomparisons. *J. Atmos. Ocean. Technol.* **40**, 455–473 (2023).
37. Yang, C. et al. Sea surface temperature intercomparison in the framework of the Copernicus Climate Change Service (C3S). *J. Clim.* **34**, 5257–5283 (2021).
38. Zhang, X., Zhao, N., Han, Z. & Dai, Z. Large spread in marine heatwave assessments for Asia and the Indo-Pacific between sea-surface-temperature products. *Commun. Earth Environ.* **5**, 195 (2024).
39. Worsfold, M., Good, S., Atkinson, C. & Embury, O. Presenting a long-term, reprocessed dataset of global sea surface temperature produced using the OSTIA system. *Remote Sens.* **16**, 3358 (2024).
40. Huang, B. et al. Improvements of the Daily Optimum Interpolation Sea Surface Temperature (DOISST) Version 2.1. *J. Clim.* **34**, 2923–2939 (2021).
41. Castro, S. L., Wick, G. A. & Steele, M. Validation of satellite sea surface temperature analyses in the Beaufort Sea using UpTemp buoys. *Remote Sens. Environ.* **197**, 458–475 (2016).
42. Xu, T. et al. An increase in marine heatwaves without significant changes in surface ocean temperature variability. *Nat. Commun.* **13**, 7396 (2022).
43. Kwok, R. Arctic sea ice thickness, volume, and multiyear ice coverage: losses and coupled variability (1958–2018). *Environ. Res. Lett.* **13**, 105005 (2018).
44. Silva, E. N. S. & Anderson, B. T. Northeast Pacific marine heatwaves linked to Kuroshio Extension variability. *Commun. Earth Environ.* **4**, 367 (2023).
45. Comiso, J. C., Meier, W. N. & Gersten, R. Variability and trends in the Arctic Sea ice cover: results from different techniques. *J. Geophys. Res. Oceans* **122**, 6883–6900 (2017).
46. Meier, W. N., Fetterer, F., Windnagel, A. K. & Stewart, J. S. NOAA/NSIDC Climate Data Record of Passive Microwave Sea Ice Concentration, Version 4 [Data Set]. Boulder, Colorado USA. National Snow and Ice Data Center (2021). <https://doi.org/10.7265/efmz-2t65>.
47. Hobday, A. J. et al. A hierarchical approach to defining marine heatwaves. *Prog. Oceanogr.* **141**, 227–238 (2016).
48. Nurser, A. J. G. & Bacon, S. The Rossby radius in the Arctic Ocean. *Ocean Sci.* **10**, 967–975 (2014).
49. Sun, D., Li, F., Jing, Z., Hu, S. & Zhang, B. Frequent marine heatwaves hidden below the surface of the global ocean. *Nat. Geosci.* **16**, 1099–1104 (2023).

## Acknowledgements

We thank the following institutions for providing satellite-based products: the UK Met Office, the National Oceanic and Atmospheric Administration, and the National Snow and Ice Data Center. We thank Dr. Mark Worsfold (UK Met Office) for his kind help in explaining the details of the reprocessed OSTIA data. N.Z. is partially supported by JSPS KAKENHI (23K11403). Z.D. is supported by Shanghai International Science and Technology Cooperation Fund Project (23230713800).

## Author contributions

X.Z.: Data collection, Methodology, Data Analysis, Writing-Editing. N.Z.: Conceptualization, Data collection, Methodology, Data Analysis, Visualization, Writing-Editing. Z.D.: Conceptualization, Writing-Editing. Z.H.: Methodology, Writing-Editing.

## Competing interests

The authors declare no competing interests.

## Additional information

**Supplementary information** The online version contains supplementary material available at <https://doi.org/10.1038/s43247-025-01997-9>.

**Correspondence** and requests for materials should be addressed to Ning Zhao or Zhijun Dai.

**Peer review information** *Communications Earth & Environment* thanks the anonymous reviewers for their contribution to the peer review of this work. Primary Handling Editor: Alireza Bahadori. A peer review file is available.

**Reprints and permissions information** is available at <http://www.nature.com/reprints>

**Publisher's note** Springer Nature remains neutral with regard to jurisdictional claims in published maps and institutional affiliations.

**Open Access** This article is licensed under a Creative Commons Attribution-NonCommercial-NoDerivatives 4.0 International License, which permits any non-commercial use, sharing, distribution and reproduction in any medium or format, as long as you give appropriate credit to the original author(s) and the source, provide a link to the Creative Commons licence, and indicate if you modified the licensed material. You do not have permission under this licence to share adapted material derived from this article or parts of it. The images or other third party material in this article are included in the article's Creative Commons licence, unless indicated otherwise in a credit line to the material. If material is not included in the article's Creative Commons licence and your intended use is not permitted by statutory regulation or exceeds the permitted use, you will need to obtain permission directly from the copyright holder. To view a copy of this licence, visit <http://creativecommons.org/licenses/by-nc-nd/4.0/>.

© The Author(s) 2025